Pharmaceutical Research, Vol. 3, No. 2, 1986

Review

Fundamentals of Powder Compression. II. The Compression of Binary Powder Mixtures[1,2]

Hans Leuenberger[3] and Bhagwan Dass Rohera[3,4]

Although tablet formulations are multicomponent systems, there have been only a few studies on the compression of binary or ternary powder mixtures. Physical interactions between the individual components may influence important biopharmaceutical properties of the compact, e.g., disintegration time and dissolution rate of the active ingredient. In the second part of this review paper the importance of these physical interactions is emphasized. The investigations are limited to the strength of the compact. An attempt is made to deduce additivity rules for the material-specific compressibility and compactibility parameters. Such additivity rules are of special importance, as they may allow the prediction of tablet properties at the formulation test. The final section is devoted to problems in compression, i.e., sticking and capping.

KEY WORDS: compression; compressibility; compactibility; binary powder mixtures; additivity rules; strength of a compact; sticking; capping.

BINARY MIXTURES

Compactibility and Compressibility of Binary Mixtures

Leuenberger (1,3) assumed that the theory of bonding and nonbonding contact points should also apply to powder mixtures. Therefore, for binary mixtures consisting of components A and B at a ratio x and $(1 - x)$, respectively (weight percentages), Eq. (7) can be written as

$$P_{\text{mixture}} = P_{\max_{\text{mixture}}} [1 - \exp(-\gamma_{\text{mixture}}\, \sigma_c \rho_4)] \quad (27)$$

Since the relative change in the deformation hardness dP of the compact is a function of the applied compression stress σ_c and change in relative density $d\rho_r$, Eqs. (7) and (27) can be differentiated for individual components A and B and for their binary mixture in the following form:

$$\frac{dP_A}{d(\sigma_c \rho_r)} = \gamma_A P_{\max_A} \exp(-\gamma_A \sigma_c \rho_r) \quad (28)$$

$$\frac{dP_B}{d(\sigma_c \rho_r)} = \gamma_B P_{\max_B} \exp(-\gamma_B \sigma_c \rho_r) \quad (29)$$

and

$$\frac{dP_{\text{mixture}}}{d(\sigma_c \rho_r)} = \gamma_{\text{mixture}} P_{\max_{\text{mixture}}} \exp(-\gamma_{\text{mixture}}\, \sigma_c \rho_r) \quad (30)$$

According to the original derivation of the equation for pure substances, it is necessary for these partial derivatives to have an identical form for pure substances as well as for binary mixtures.

In the limiting case of pure component A or B, $dP_{\text{mixture}}/d(\sigma_c \rho_r)$ should be equal to $dP_A/d(\sigma_c \rho_r)$ or $dP_B/d(\sigma_c \rho_r)$ respectively.

This is, however, possible only in the case where a logarithmic mean of partial derivatives is taken, i.e.,

$$\frac{dP_{\text{mixture}}}{d(\sigma_c \rho_r)} = \left(\frac{dP_A}{d(\sigma_c \rho_r)}\right)^x \left(\frac{dP_B}{d(\sigma_c \rho_r)}\right)^{(1-x)} \quad (31)$$

Assuming that this holds true, Eq. (19) can be written as

$$\frac{dP_{\text{mixture}}}{d(\sigma_c \rho_r)} = \gamma_A^x \gamma_B^{(1-x)} P^x_{\max_A} P^{(1-x)}_{\max_B} \exp\{-[x\gamma_A + (1 - x)\gamma_B]\sigma_c \rho_r\} \quad (32)$$

Integration of Eq. (32) leads to the following compression equation for binary mixtures:

$$P_{\text{mixture}} = \frac{P^x_{\max_A} P^{(1-x)}_{\max_B} \gamma_A^x \gamma_B^{(1-x)}}{x\gamma_A + (1 - x)\gamma_B} \{1 - \exp[-(x\gamma_A + (1 - x)\gamma_B)\sigma_c \rho_r]\} \quad (33)$$

where P_{mixture} is the deformation hardness of the compact of the binary mixture of components A and B, $P_{\max_A}$ is the maximum deformation hardness of the compact of component A, $P_{\max_B}$ is the maximum deformation hardness of the compact of component B, γ_A is the compression suscepti-

[1] The first part of this paper, "Fundamentals of Powder Compression. I. The Compactibility and Compressibility of Pharmaceutical Powders," was published in the preceding issue of this journal [*Pharm. Res.* 3(1):12–22 (1986)]. The numbering of equations, references, figures, and tables herein is a continuation of that from the previous paper.

[2] This paper is derived from a series of lectures held at the Intensive Course on Agglomeration at the Department of Chemical Engineering, University of Waterloo, Waterloo, Ontario, Canada, May 30–June 1, 1985.

[3] School of Pharmacy, University of Basle, CH-4051 Basle, Switzerland.

[4] Present address: The Philadelphia College of Pharmacy and Science, 43rd Street and Kingsessing Mall, Philadelphia, Pennsylvania 19104.

0724-8741/86/0400-0065$05.00/0

bility of component A, γ_B is the compression susceptibility of component B, x is the proportion of component A, $(1 - x)$ is the proportion of component B, σ_c is the compression stress applied to make the compact, and ρ_r is the relative density of the compact.

According to Eq. (33), the following additivity rules for the compactibility and compressibility parameters were derived.

$$\ln P_{max_{mixture}} = x \ln P_{max_A} + (1 - x) \ln P_{max_B} + \ln \frac{\gamma_A^x \gamma_B^{(1-x)}}{x\gamma_A + (1 - x)\gamma_B} \quad (34)$$

or approximative for $\gamma_A \sim \gamma_B$:

$$\ln P_{max_{mixture}} \cong x \ln P_{max_A} + (1 - x) \ln P_{max_A} + (1 - x) \ln P_{max_B} \quad (35)$$

and

$$\gamma_{mixture} = x\gamma_A + (1 - x)\gamma_B \quad (36)$$

These additivity rules can be generalized to take into account possible physical interaction between component A and component B of the binary mixture. In that case Eqs. (35) and (36) can be expanded to

$$\ln P_{max_{mixture}} = x \ln P_{max_A} + (1 - x) \ln P_{max_B} + x(1 - x) \ln P_{ww} \quad (37)$$

and

$$\gamma_{mixture} = x\gamma_A + (1 - x)\gamma_B + x(1 - x)\gamma_{ww} \quad (38)$$

where P_{ww} is the interaction term for the compactibility parameter and γ_{ww} is the interaction term for the compressibility parameter.

If there is no interaction in terms of compactibility and compressibility, then

$$\ln P_{ww} = 0, \text{ i.e., } \quad P_{ww} = 1$$

and

$$\gamma_{ww} = 0$$

However, in case of a positive interaction,

$$\ln P_{ww} > 0, \quad \text{i.e., } P_{ww} > 1$$

and

$$\gamma_{ww} > 0$$

And in case of a negative interaction,

$$\ln P_{ww} < 0, \quad \text{i.e., } 0 < P_{ww} < 1$$

and

$$\gamma_{ww} < 0$$

All three types of interactions have been reported. Leuenberger (3) observed negative interaction in a lactose–sucrose binary system. Jetzer *et al.* (34,110) have reported negative interaction in aspirin–Emcompress and Avicel–lactose, positive interaction in potassium bromide–potassium chloride, and zero or no interaction in aspirin–metamizol and aspirin–caffeine binary systems.

Mathematical Relationship Between P_{max} and γ

Leuenberger has shown that at low compression stress, the deformation hardness P of the compact is much less than the maximum deformation hardness P_{max} which it attains at a very high or infinite compression stress σ_c. Accordingly, its relative density ρ_r is less than unity. This can be expressed as follows.

At low compression stress,

$$P \ll P_{max} \quad (39)$$

and

$$\sigma_c \rho_r \ll 1/\gamma \quad (40)$$

In that case, Eq. (7) can be simplified to

$$P \cong (P_{max}\gamma)\sigma_c\rho_r \quad (41)$$

where P is a linear function of $\sigma_c\rho_r$ with slope value $P_{max}\gamma$, i.e.,

$$P_{max}\gamma = a \text{ (dimensionless constant)} \quad (42)$$

or

$$P_{max} = \frac{a}{\gamma} \quad (43)$$

or

$$\gamma = \frac{a}{P_{max}} \quad (44)$$

where a is the slope of the linear function of P against $\sigma_c\rho_r$.

Equation (44) shows the "flip-flop" problem of estimating P_{max} and γ independently; e.g., in a nonlinear regression analysis, an underestimate of γ corresponds to an overestimate of P_{max}. Thus one observes a correlation between P_{max} and γ, which is valid for any compression stress.

This correlation can be easily shown for a set of binary mixtures, where

$$P_{max} = \frac{a}{\gamma} + b \text{ (intercept)} \quad (45)$$

This relationship shows that the P_{max} value of individual components and their binary mixtures, when plotted against the reciprocal of the compressibility parameter γ, would yield a straight line with slope a, passing through the origin, i.e., intercept $b = 0$.

However, in practice, the straight line may not pass through the origin, which introduces a systemic error. In that case, if $b \ll P_{max}$, it can be neglected.

Substituting Eq. (44) in Eq. (33),

$$P_{max_{mixture}} \cong P_{max_A}^x P_{max_B}^{(1-x)} \frac{a^x a^{(1-x)}}{P_{max_A}^x P_{max_B}^{(1-x)}} \frac{1}{\frac{xa}{P_{max_A}} + \frac{(1 - x)a}{P_{max_B}}} \quad (46)$$

and simplifying, one obtains

$$P_{max_{mixture}} \cong \frac{P_{max_A} P_{max_B}}{xP_{max_B} + (1 - x) P_{max_A}} \text{ (harmonic mean)} \quad (47)$$

Using the approximate Eq. (47), the interaction $I(x)$ can be defined as deviation from linear additivity as follows:

$$I(x) = xP_{\max_A} + (1 - x)\,P_{\max_B} - H(P_{\max_A}, P_{\max_B}) \tag{48}$$

or

$$I(x) \cong \frac{x(1 - x)}{P_{\max_A} P_{\max_B}} (P_{\max_A} - P_{\max_B})^2 H(P_{\max_A}, P_{\max_B}) \tag{49}$$

where $I(x)$ is the interaction term for the compactibility parameter representing deviation from linear additivity, $P_{\max_{mixture}}$ is the maximum deformation hardness of the compact of the binary mixture of components A and B, $P_{\max_A}$ is the maximum deformation hardness of the compact of component A, $P_{\max_B}$ is the maximum deformation hardness of the compact of component B, x is the proportion of component A, $(1 - x)$ is the proportion of component B, and H is the harmonic mean.

Statistical Model Approach for Powder Mixtures

Although powders differ from liquids in that they are heterogeneous, consisting of discrete solid particles of different sizes and shapes interspersed with void spaces, they are similar to liquids in that they deform and flow when stressed (111). It is not surprising therefore that in binary powder systems, physical interactions similar to those in solutions may occur.

According to a statistical approach (112), fraction x of a component in a powder system represents its distribution probability; and the probability of having a like particle as a neighbor is proportional to x^2. Considering these assumptions, different statistical weights can be attributed to the different possible interactions:

Interaction	A–A	A–B	B–A	B–B
Statistical weight	x^2	$x(1 - x)$	$x(1 - x)$	$x(1 - x)^2$

This approach is also used to describe interactions of impurities in the crystal lattice (113).

The statistical approach can therefore be used to establish the following relationship between the compactibility parameter $P_{\max}$ of individual components A and B and their binary mixtures:

$$\ln P_{\max_{mixture}} = x^2 \ln P_{\max_A} + 2x(1 - x) \ln P_{\max_{AB}} + (1 - x)^2 \ln P_{\max_B} \tag{50}$$

i.e.,

$$P_{\max_{mixture}} = x \ln P_{\max_A} + (1 - x) \ln P_{\max_B} + x(1 - x)\,[2 \ln P_{\max_{AB}} - (\ln P_{\max_A} + \ln P_{\max_B})] \tag{51}$$

One observes that Eq. (51) is identical to Eq. (37), i.e.,

$$\ln P_{\max_{mixture}} = x \ln P_{\max_A} + (1 - x) \ln P_{\max_B} + x(1 - x) \ln P_{WW} \tag{37}$$

Thus the interaction term can be represented as

$$\ln P_{WW} = \ln \frac{P_{\max_{AB}}^2}{P_{\max_A} P_{\max_B}} \tag{52}$$

where $P_{\max_{mixture}}$ is the maximum deformation hardness of the compact of the binary mixture of components A and B, $P_{\max_A}$ is the maximum deformation hardness of the compact of component A, $P_{\max_B}$ is the maximum deformation hardness of the compact of component B, P_{WW} is the interaction term for the compactibility parameter, x is the proportion of component A, and $(1 - x)$ is the proportion of component B.

It should be emphasized that, in this derivation, $P_{\max_{AB}}$ is not identical to $P_{\max_{mixture}}$ but describes the physical interaction between two components on a molecular level, i.e., the interaction (energy/volume) between two neighboring unlike molecules:

For the limiting case when $P_{\max_A} = P_{\max_B} = P_{\max_{AB}}$,

$$\ln P_{WW} = 0 \tag{53}$$

For other cases,

$$\ln P_{WW} > 0, \quad \text{i.e., positive interaction} \rightarrow P_{\max_{AB}}^2 > P_{\max_A} P_{\max_B} \tag{54}$$

or

$$\ln P_{WW} < 0, \quad \text{i.e., negative interaction} \rightarrow P_{\max_{AB}}^2 < P_{\max_A} P_{\max_B} \tag{55}$$

The interaction term $\ln P_{WW}$ could recently be related to the difference in solubility parameters of the corresponding solids (121).

The Compactibility and Compressibility of Binary Powder Mixtures Consisting of Brittle and Soft Materials

In order to study the compaction behavior of binary powder systems consisting of components of dissimilar deformation properties and to determine, qualitatively and

Table V. Physical Characteristics of the Powder Material

Substance	Poured density (g/cm³)	Tapped density (g/cm³)	Particle size analysis (RRS-B distr.) n	Particle size analysis (RRS-B distr.) d (μm)	Loss on drying (%, w/w)	Surface area (cm²/g)
Caffeine	0.331	0.476	2.43	34.0	0.1	5200
Magnesium stearate	0.184	0.347	2.46	32.3	2.5	26,800
Polyethylene glycol 4000	0.516	0.725	2.82	45.7	0.4	1800
Sodium lauryl sulfate	0.192	0.269	3.11	39.8	0.5	18,000
Sodium stearate	0.250	0.431	2.68	34.9	1.5	17,300

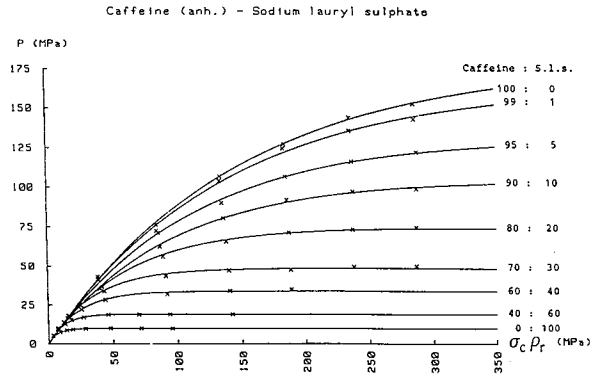

Fig. 7a. Plot of deformation hardness (P) against the product of compression stress (σ_c) and relative density (ρ_r) for various composition ratios (w/w).

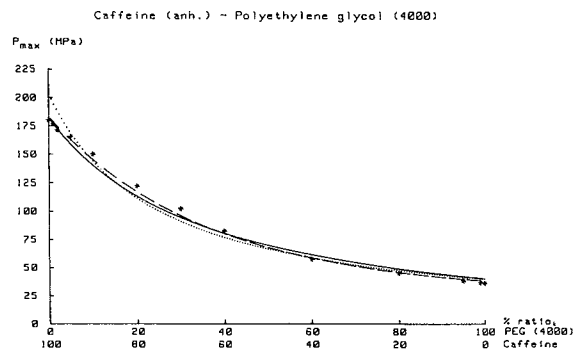

Fig. 8b. P_{max} values (*) determined according to Eq. (7) for the individual binary mixtures and graphical representation of Eqs. (33) (——), (37) (— —), and (47) (····).

quantitatively, the physical interaction between these components, the following mixtures were investigated.

Brittle material	Plastic material
Caffeine (anhydrous) powder	Magnesium stearate
Caffeine (anhydrous) powder	Polyethylene glycol (4000)
Caffeine (anhydrous) powder	Sodium lauryl sulfate
Caffeine (anhydrous) powder	Sodium stearate

In the first phase of evaluation, the compactibility parameter P_{max} and the compression susceptibility or compressibility parameter γ of single components and their binary mixtures were computed individually by the basic model Eq. (7). In the second phase, data for all composition ratios were simultaneously evaluated by either the exact model Eq. (33) or the additivity rules Eqs. (36) and (37) or Eqs. (36) and (47) for binary mixtures. The evaluations were performed using nonlinear regression analysis.

The physical characteristics of the starting material are summarized in Table V.

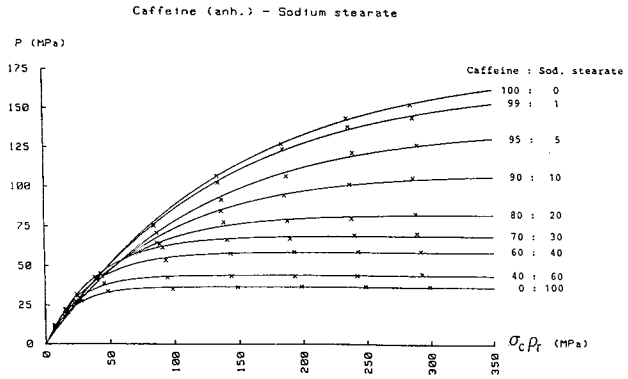

Fig. 7b. Plot of deformation hardness (P) against the product of compression stress (σ_c) and relative density (ρ_r) for various composition ratios.

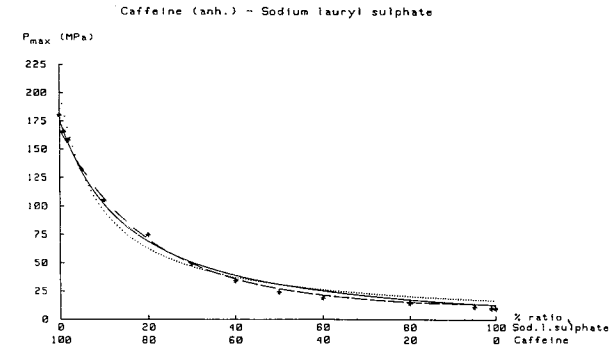

Fig. 8c. P_{max} values (*) determined according to Eq. (7) for the individual binary mixtures and graphical representation of Eqs. (33) (——), (37) (— —), and (47) (····).

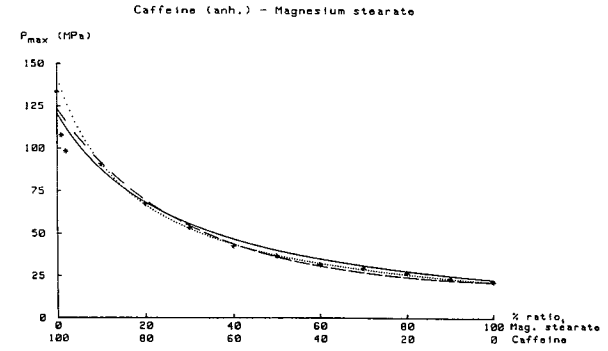

Fig. 8a. P_{max} values (*) determined according to Eq. (7) for the individual binary mixtures and graphical representation of Eqs. (33) (——), (37) (— —), and (47) (····).

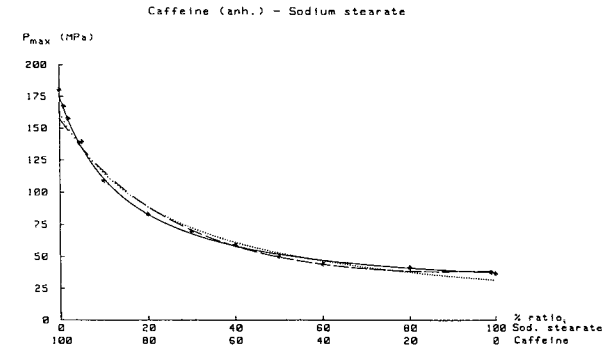

Fig. 8d. P_{max} values (*) determined according to Eq. (7) for the individual binary mixtures and graphical representation of Eqs. (33) (——), (37) (— —), and (47) (····).

Individual Estimation of Compression Parameters

Typical plots of compaction profiles of individual components and their binary mixtures are shown in Figs. 7a and b. For clarity, the results of only selected binary mixtures are shown. A diagrammatic representation of the compactibility parameter P_{max} and compressibility parameter γ against the ratio of components (weight/weight) in the mixtures are shown in Figs. 8a–d and 9a–d, respectively. The P_{max} values in Figs. 8a–d adequately follow the additivity rules according to the exact equation [Eqs. (33) and (34), respectively] and Eq. (37) introducing the interaction term P_{ww} and according to the harmonic-mean Eq. (47). A model discrimination based on differences in the minima of the sum of squares calculated by the nonlinear regression analysis is not possible. The compressibility parameter γ, however, estimated for single components as well as for their binary mixtures, when plotted against the ratio of components in the mixture, exhibited a trend of two straight lines that intersect each other (see Figs. 9a–d). The regression coefficient of each line exceeded 0.99. The point of intersection, or critical composition ratio X^*, varied in individual systems and was observed at ~25% polyethylene glycol (4000) or sodium lauryl sulfate, ~35% magnesium stearate, and ~60% sodium stearate composition (by weight) in the respective binary systems.

This behavior of the compressibility parameter γ of binary mixtures is different from that reported by Leuenberger (3) and Jetzer *et al.* (110). These authors obtained a rectilinear relationship between the γ value and the ratio of components in the mixture for a number of binary systems consisting of components of similar as well as dissimilar deformation properties.

Nevertheless, the two straight lines, each with regression coefficients better than 0.99, intersecting each other are in agreement with Leuenberger's compression theory [see Eq. (36), according to which the compressibility of powder materials is an additive property, and therefore, the compressibility of a mixture would be the arithmetic sum of the relative proportions of its components].

Since the investigated binary systems consisted of components of extremely dissimilar compaction behavior, i.e., brittle and plastic, the trend of two straight lines intersecting each other at a point indicates a process of phase inversion in which one component dominates the other one up to a critical composition ratio. Further addition of the other component seems to lead to phase inversion. The critical composition ratio X^*, at which phase inversion is observed, depends upon the physicochemical properties of individual components in the mixture. The behavior of phase inversion can be compared with that of emulsions in which, beyond a critical ratio of two immiscible liquids, further addition of liquid comprising the internal phase leads to phase inver-

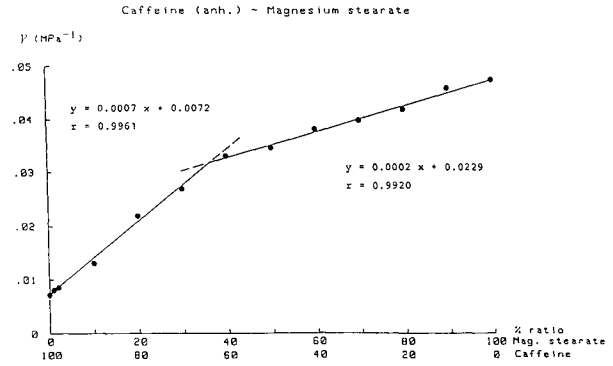

Fig. 9a. Relation between compression susceptibility or compressibility parameter γ and composition ratio (w/w). (●) Compressibility parameter γ estimated for each composition ratio separately by means of basic Eq. (7).

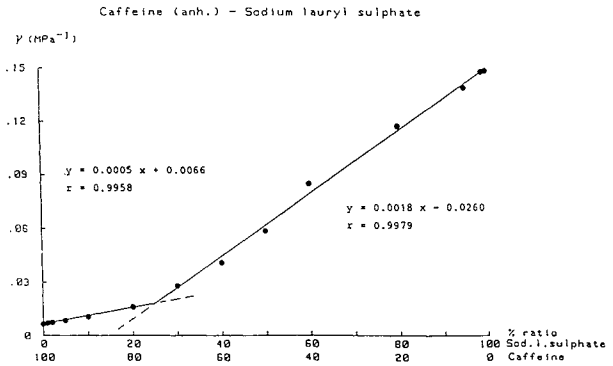

Fig. 9c. Relation between compression susceptibility or compressibility parameter γ and composition ratio (w/w). (●) Compressibility parameter γ estimated for each composition ratio separately by means of basic Eq. (7).

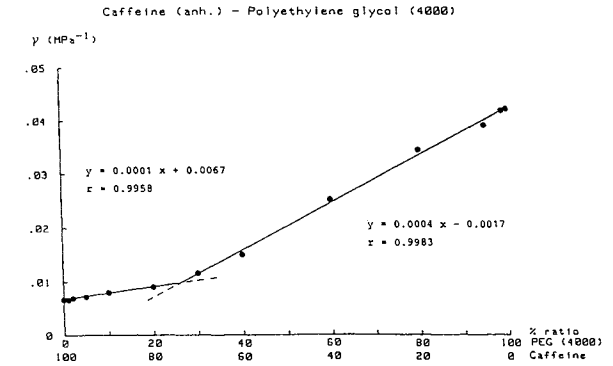

Fig. 9b. Relation between compression susceptibility or compressibility parameter γ and composition ratio (w/w). (●) Compressibility parameter γ estimated for each composition ratio separately by means of basic Eq. (7).

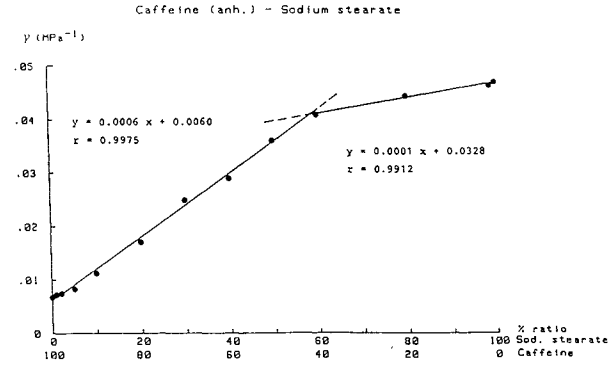

Fig. 9d. Relation between compression susceptibility or compressibility parameter γ and composition ratio (w/w). (●) Compressibility parameter γ estimated for each composition ratio separately by means of basic Eq. (7).

sion, i.e., inversion of the internal phase into the outer phase.

Figures 7a and 7b present qualitative evidence of the trend of phase inversion in various binary systems. In these diagrams, the shape of the compaction curve, which is suggestive of the compaction behavior of powder material under pressure, shows a predominance of one component over the other up to a certain composition ratio. With respect to the individual system, the change in the shape of the curve is conspicuous at or around its critical composition ratio X^*, at which phase inversion in compression susceptibility or compressibility is observed.

Under the assumption of phase inversion, it is observed that in the case of the caffeine–polyethylene glycol (4000) and caffeine–sodium lauryl sulfate systems, caffeine dominates the system up to ~25% of the plastic component in the respective binary system. Beyond this critical composition ratio, a phase inversion is observed and the plastic component starts dominating the system (see Figs. 9b and c).

The assumption of phase inversion was supported by surface characteristics of tablets seen with the scanning electron microscope (Stereoscan mark 2A, Cambridge Scientific Instruments, Cambridge, England). Figure 10 shows photomicrographs of the upper surface of tablets of caffeine–sodium lauryl sulfate binary mixtures compressed at 154.84–MPa pressure. All the photomicrographs were taken at 100× magnification under constant conditions and exhibit dark and bright patches which have been identified as caffeine and sodium lauryl sulfate particles, respectively. It is evident from these photomicrographs that sodium lauryl

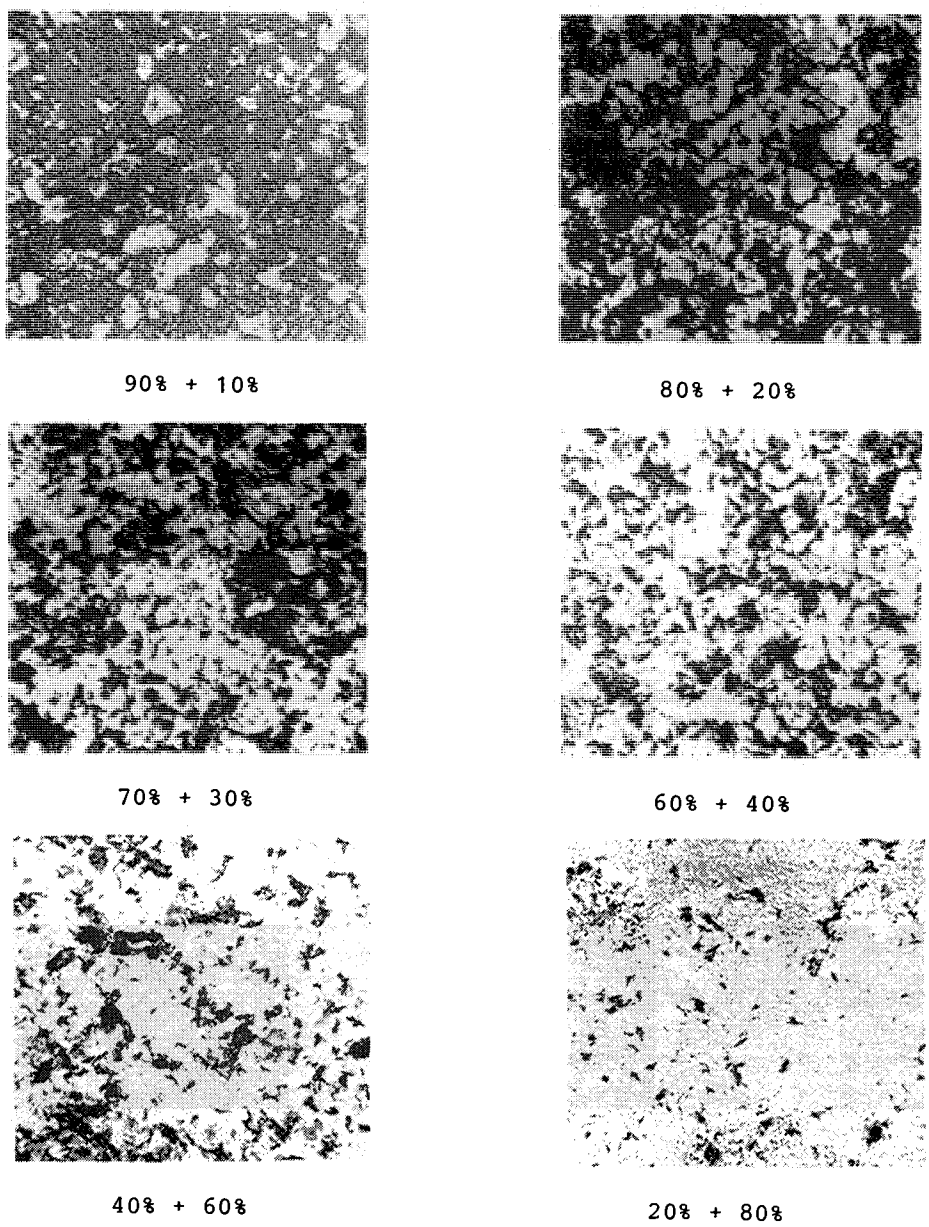

Fig. 10. Scanning electron micrographs of surfaces of caffeine (anh.)–sodium lauryl sulfate mixture tablets compressed at 154.84-MPa pressure. Tablet composition shown is percentage (w/w) caffeine and sodium lauryl sulfate, respectively. 100×; reduced 20% for reproduction.

sulfate, which undergoes plastic deformation under pressure, is smeared on the tablet surface and occupies a relatively larger surface area than its relative proportion in the mixture. Beyond a 20 to 30% sodium lauryl sulfate composition in the mixture, caffeine seems to be encapsulated, and the tablet surface is almost covered with sodium lauryl sulfate when it starts dominating the system and a phase inversion takes place.

Sodium lauryl sulfate and caffeine in the tablets were identified by an energy dispersive X-ray analyzer (EDAX Model 707, EDAX International Inc., Chicago). Sodium lauryl sulfate was identified by a prominent identification peak of K_α shell of sulfur, whereas caffeine, having no detectable element, did not give any identification peak. Figures 11a and b show EDAX diagrams of sodium lauryl sulfate and caffeine, respectively.

In the caffeine–polyethylene glycol (4000) binary system, it was observed that at lower compression pressures, i.e., ~52 MPa and less, the tablet porosity varied linearly with the relative proportion of the individual components in the mixture. This is in agreement with the results of Ramaswamy *et al.* (122), who demonstrated that the total porosity of a consolidated binary mixture is the sum of porosities of the two components when compacted. However, at higher compression stresses, i.e., ~155 MPa and more, a conspicuous change in tablet porosity was observed at ~30% polyethylene glycol (4000) composition. Figures 12a and b show plots of the theoretically predicted and practically observed porosity in tablets, compressed at 51.61- and 154.84-MPa pressures, against the component ratio in the binary mixture. Since compressibility is a relative density- or porosity-specific property, a conspicuous change in tablet porosity at an ~30% polyethylene glycol (4000) composition supports the observation of change in the compressibility at this composition ratio.

A comparison of the caffeine–polyethylene glycol (4000) and caffeine–sodium lauryl sulfate systems shows that with up to an ~25% polyethylene glycol (4000) composition in the mixture, a change in the compressibility of the system is practically negligible, whereas sodium lauryl sulfate shows a change even at compositions lower than 25%. This fact is evident from the γ values as well as from the slope value of the plot of the compressibility parameter γ against the ratio of components in the respective binary system (see Figs. 9b and c); the slope value with up to an ~25% polyethylene glycol (4000) composition in the mixture is lower than that with the same composition ratio of sodium

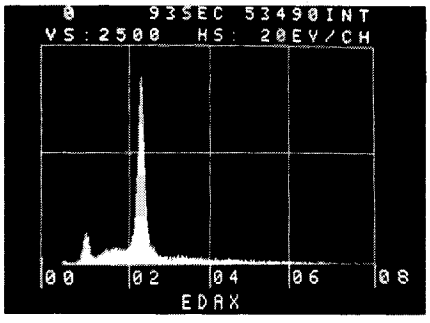

Fig. 11a. EDAX diagram for the identification of sodium lauryl sulfate.

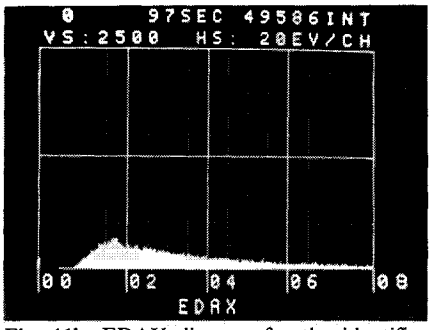

Fig. 11b. EDAX diagram for the identification of caffeine. Identification of bright and dark patches observed in Fig. 14 as sodium lauryl sulfate and caffeine (anh.) particles, respectively, by energy dispersive X-ray spectrometry (EDAX).

lauryl sulfate. Among other factors, this effect can be attributed to the difference in the specific surface area of the two substances; the specific surface area of sodium lauryl sulfate is almost 10 times larger than that of polyethylene glycol (4000) (see Table V).

In contrast, magnesium stearate and sodium stearate show an increase in the compressibility of the binary system even at low concentrations. In the case of magnesium stearate, a steep increase in the compressibility is observed up to a content of ~35% in the binary system (see Fig. 9a). This indicates that the influence of magnesium stearate starts at a very low content, and after a critical composition ratio X^* ~35%, it dominates the external phase exclusively. A further

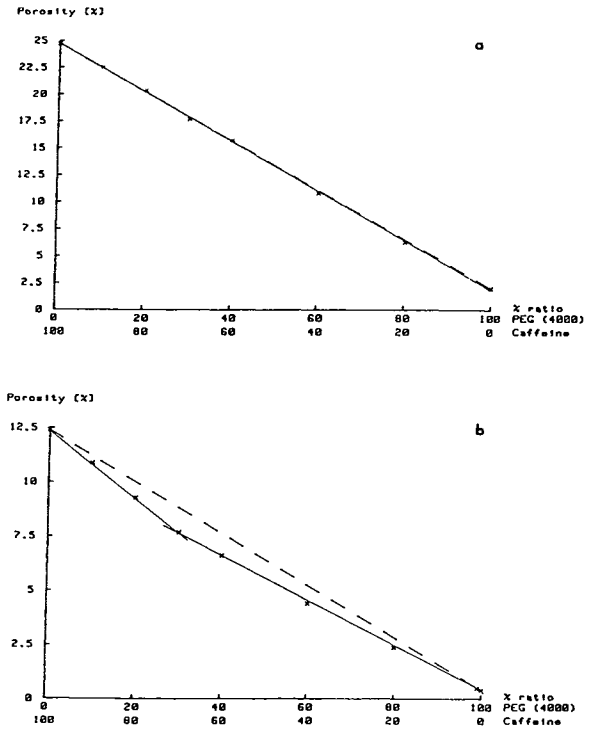

Fig. 12. Plot of tablet porosity against composition (w/w) of caffeine (anh.)–polyethylene glycol (4000) binary mixtures compressed at (a) 51.61-MPa and (b) 154.84-MPa pressures. (——) Observed porosity; (— — —) predicted porosity.

increase in the magnesium stearate composition shows little effect on the compressibility of the system. Similar behavior is observed in the caffeine–sodium stearate binary system. However, sodium stearate dominates the system only above ~60% in the mixture (see Fig. 9d).

It is not surprising to observe that, in terms of compression susceptibility or the compressibility parameter γ, polyethylene glycol (4000) and sodium lauryl sulfate exhibit a different behavior than magnesium stearate and sodium stearate. In the case of polyethylene glycol (4000) and sodium lauryl sulfate, there is initially little change in the compressibility up to an ~25% content in the respective system, after which there is a steep rise. In contrast, magnesium stearate and sodium stearate contribute to the compressibility even at low composition ratios, and after ~35 and ~60% contents in the mixture, respectively, cease to show any further change.

This difference is apparently due to the fact that hydrophobic lubricants, especially salts of stearic acid, are more effective boundary lubricants even at low concentrations, owing to the virtue of their low shear strength, ability to adhere to the particle surface, and toughness in film formation. On the contrary, synthetic soluble wax-like polymers, typified by polyethylene glycols (PEGs), and other hydrophilic lubricants are less effective at low concentrations.

The trend of phase inversion seems to be specific to the systems consisting of components of dissimilar deformation properties and is assumed to be a function of compression stress and powder variables, e.g., particle size, shape, packing characteristics, etc. A detailed investigation of these powder variables exceeds the scope of the present work, but they will be studied in the future. The question remains open how the particle size and the specific surface area of components of the system influence the magnitude of physical interaction in terms of compactibility, i.e., P_{WW}, and consolidation behavior, i.e., the critical composition ratio X^* at which one component starts dominating the other in a binary system.

PROBLEMS IN COMPRESSION

Sticking

The expression "sticking" generally means that the compact sticks to the punch surface, i.e., upper punch or lower punch. Another type of sticking occurs within the die. Qualitatively, both types of sticking are related to the fact that the adhesive forces at the punch or die-wall surfaces dominate the cohesive forces in the material to form the compact. Problems of sticking can be overcome by changing the formulation (i.e., adding antisticking agents, changing the amount or type of lubricant in case of die-wall sticking, and correctly polishing the punch and die-wall surfaces. The sticking tendency of a formulation can be measured experimentally, using instrumental tableting machines (114). Thus the force to separate the tablet from the lower punch can be quantified. To check the performance of the lubricant, force transmission from the upper to the lower punch can be measured. There is also a possibility of monitoring the ejection forces during removal of the tablet from the die. It is known that the stress distribution in the compact is rather inhomogeneous (115) and depends on the concentration of the lubricant (116).

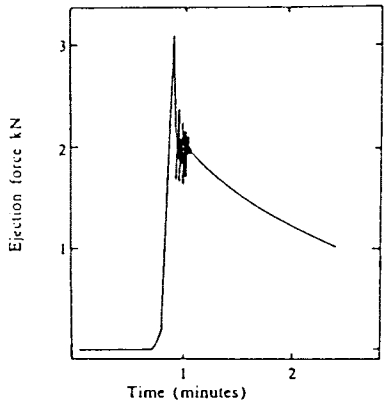

Fig. 13. Typical trace for the ejection of unlubricated potassium chloride, 420- to 495-μm fraction, compressed to 57.3 MNm^{-2} and ejected at 1 mm min^{-1}.

$$\sigma_z(l) = \sigma_{z_0} e^{-4\mu\nu\, l/d} \tag{56}$$

where σ_z is the axial compressional stress as a function of the depth l in the cylindrical compact, σ_{z0} is the compressional stress at $l = 0$ (i.e., at the upper punch level), d is the diameter of the cylindrical compact, μ is the friction coefficient, and ν is the Poisson number (ratio between radial and axial stress). During the ejection of the tablet slip-stick effects may occur (117) (see Fig. 13).

Capping

With a capping tendency, the compact may break in the die after decompression or during the ejection process. Brittle material shows a distinct capping tendency. During the compression of powder systems, a work-hardening process is usually present. Thus, originally soft material may become brittle. In practice, it was found that differences in the dimensions of punch and die diameter may play an important role. The idea was put forward that compressed air having difficulty escaping from the die is responsible. It is known today that differences in the dimensions of the punch and die diameters together with the lubricant concentration influence stress distribution in the compact material. This stress distribution during decompression and the type of stress relief are responsible for the occurrence of a possible capping. Residual stress in the die can easily be shown on the basis of compression and decompression of a Long body (118). At a low compressional stress, the Long body shows perfect elastic behavior. Therefore, the radial stress σ_r is proportional to the axial stress σ_z (see Fig. 14).

$$\sigma_r = \nu\, \sigma_z, \qquad 0 < \nu < 0.5 \tag{57}$$

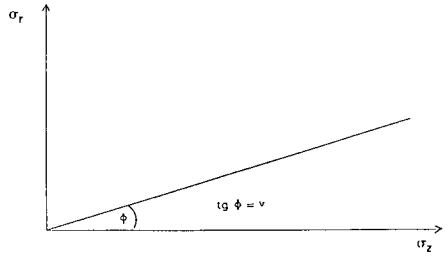

Fig. 14. Perfect elastic behavior.

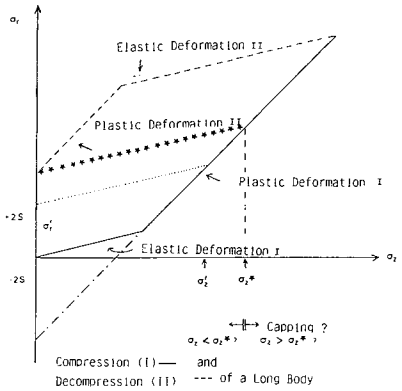

Fig. 15. Compression and decompression of a Long body.

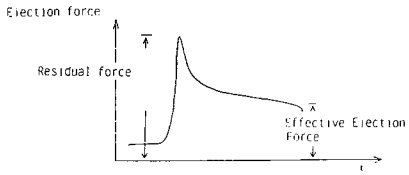

Fig. 16. Residual force and effective ejection force.

where ν is the Poisson number. Plastic deformation starts as soon as the difference betwen axial and radial stress exceeds $2S$ (= yield stress).

$$\sigma_z - \sigma_r = 2S \tag{58}$$

This equation represents the flow criterion for a Long body. We assume that we have an instrumental press and that we simultaneously measure the axial stress (compressional stress due to punch) and the radial stress (die-wall pressure). The change in axial and radial stress during compression and decompression is shown in Fig. 15.

It is evident that after decompression there is a residual stress in the die. Thus the compact may relieve the stress by brittle fracture, i.e., by capping or lamination in the die. Stress relaxation may also take place by elastic deformation and/or plastic flow. An elastic expansion in radial direction is, however, only possible after removal from the die. Thus brittle fracture may also occur during ejection of the tablet. During compression, decompression, and ejection of the tablet (see Fig. 16), the stress in the compact is often locally concentrated to a large extent. Whether capping takes place or not depends on the properties of the material compressed. Brittleness of the material is a prerequisite for capping. Hiestand *et al.* (119) introduced a brittle fracture propensity test for pharmaceutical powders. For this purpose, two cubic compacts are made from the powder, alike in their dimensions, but one compact has a spherical hole. The tensile strength of these compacts is measured using the diametrical compression test (Brazilian test). Stress concentration takes place during the test at the hole of the compact (see Fig. 17). From theory it is known that at the hole, externally applied stress is amplified by a factor of three. Thus in the case of an extremely brittle material the tensile strength σ_{t_0} of the compact with the hole is reduced by a factor of three compared with the tensile strength σ_t of the compact without the hole. Consequently, Hiestand *et al.* defined the brittle fracture propensity (BFP) index as follows:

$$\mathrm{BFP} = \frac{1}{2}\left(\frac{\sigma_t}{\sigma_{t_0}} - 1\right) \tag{59}$$

Depending on the material, BFP values between approximately 0 and 1 can be determined. Capping tendency of

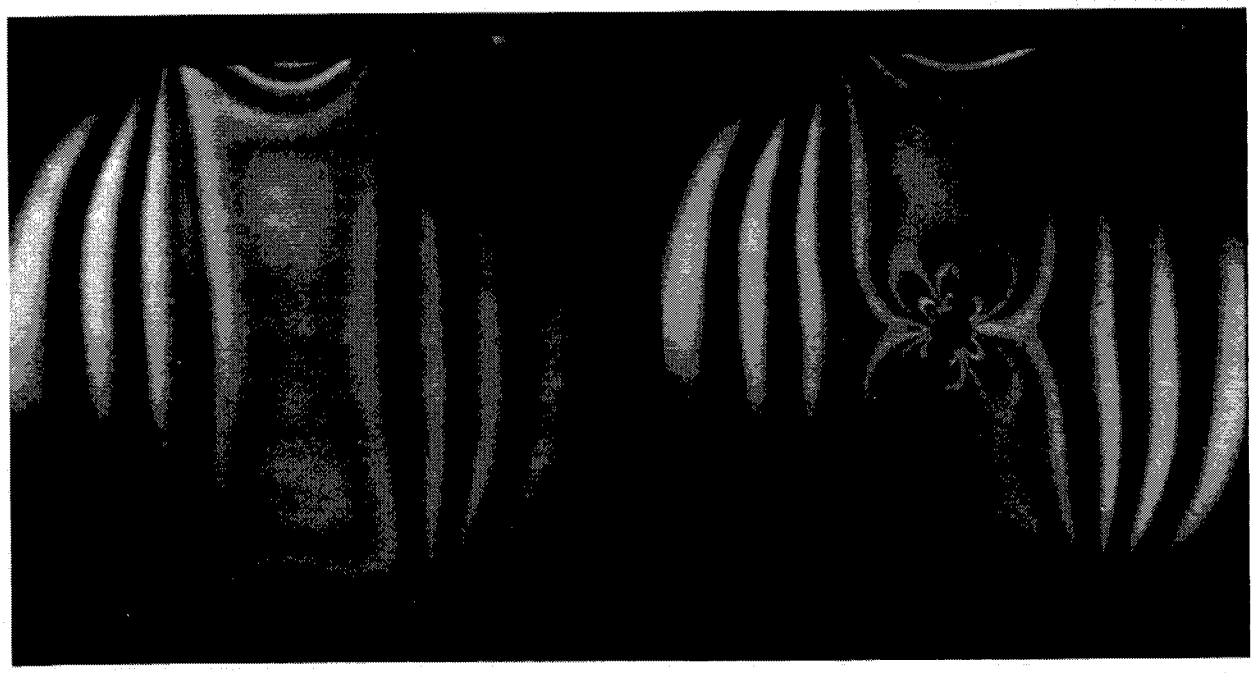

Fig. 17. Examples of simple fringe patterns obtained with and without a hole in a compact subjected to transverse compression. These photographs were made with white light and simple polarizers and are not suitable for stress analysis use. (Reproduced from Ref. 119.)

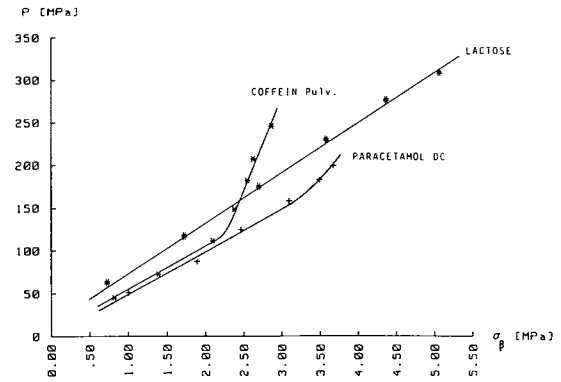

Fig. 18a Deformation hardness P plotted against tensile strength hardness σ_β (78).

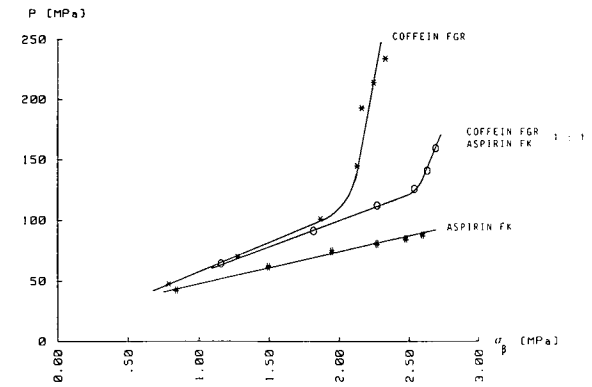

Fig. 18b. Deformation hardness P plotted against tensile strength hardness σ_β (78).

the material has to be expected for BFP values close to 1. It must be stated that the capping tendency of a material not only is a material property but also depends on the details of the compression/decompression cycle, which is a property of the machine used. Amidon *et al.* (120) showed that using a tableting press capable of triaxial decompression, no capping occurs even if rather brittle material is compressed. Similar results should be obtained using the technique of isostatic compression. Recently, in addition to the BFP index, Hiestand introduced the strain and bonding index of a compressed powder bed (79). The strain index quantifies the elastic property, i.e., the elastic energy stored per unit volume, and the bonding index quantifies the strength of bonding at the area of contact between particles in the compact. The bonding index BI corresponds to the ratio of tensile strength σ_β divided by deformation hardness P

$$\mathrm{BI} = \frac{\sigma_\beta}{P} \tag{60}$$

As shown by Hiestand *et al.* (79), the BI index is sensitive to the capping tendency of a material. Thus a sudden change in the bonding index of a powder system compressed at different compression stresses indicates a capping tendency (78) (see Fig. 18). It may be assumed that the deformation hardness test is a "local hardness test" and not sensitive to stresses and cracks in the compact, whereas the tensile strength test is a "global hardness test," influenced by cracks or stresses present in the compact. According to today's knowledge, it is questionable how many parameters are necessary for a complete description of the compression process and compression behavior of a chosen powder (79,123,124).

REFERENCES

110. W. Jetzer, H. Leuenberger, and H. Sucker. *Pharm. Technol.* 7(11):33–48 (1983).
111. P. York. *Int. J. Pharm.* 6:89–117 (1980).
112. H. D. Beyer and W. Klose. *Erdöl Kohle* 34:410 (1981).
113. K. Meyer. *Physikalisch-chemische Kristallographie,* 2nd ed., VEB Deutscher Verlag für Grundstoffindustrie, Leipzig, 1977.
114. A. Ritter, M. Dürrenberger, and H. Sucker. *Pharm. Ind.* 40:1181–1183 (1978).
115. D. Train. *J. Pharm. Pharmacol.* 8:745–761 (1956).
116. H. Unkel. *Arch. Eisenhütten Nr.* 18:161 (1945).
117. J. A. Hersey, E. T. Cole, and J. E. Rees. *Austr. J. Pharm. Sci.* NS2(1):21–24 (1973).
118. W. M. Long. *Powder Metal.* 6:73–86 (1960).
119. E. N. Hiestand, J. E. Wells, C. B. Plot, and J. F. Ochs. *J. Pharm. Sci.* 66:510–519 (1977).
120. E. Amidon, D. P. Smith, and E. N. Hiestand. *J. Pharm. Sci.* 70:613–617 (1981).
121. H. Leuenberger. *Int. J. Pharm.* 27:127–138 (1985).
122. C. M. Ramaswamy, Y. B. G. Varma, and D. Venkateswarlu. *Chem. Eng. J.* 1:168–171 (1971).
123. E. G. Rippie and D. W. Danielson. *J. Pharm. Sci.* 70:476–482 (1981).
124. D. W. Danielson, W. T. Morehead, and E. G. Rippie. *J. Pharm. Sci.* 72:342–345 (1983).